

# NH<sub>3</sub>–NO interaction at low-temperatures: An experimental and modeling study

Maria Virginia Manna<sup>a,b,\*</sup>, Pino Sabia<sup>a</sup>, Krishna P. Shrestha<sup>c</sup>,  
Lars Seidel<sup>d</sup>, Raffaele Ragucci<sup>a</sup>, Fabian Mauss<sup>c</sup>, Mara de Joannon<sup>a</sup>

<sup>a</sup> Institute of Science and Technology for Sustainable Energy and Mobility - Consiglio Nazionale delle Ricerche, Napoli, Italy

<sup>b</sup> Department of Chemical, Materials and Production Engineering - University of Napoli Federico II, Napoli, Italy

<sup>c</sup> Thermodynamics and Thermal Process Engineering - Brandenburg University of Technology, Cottbus, Germany

<sup>d</sup> LOGE Deutschland GmbH, Cottbus, Germany

Received 5 January 2022; accepted 13 September 2022

Available online 22 October 2022

## Abstract

The present work provides new insight into NH<sub>3</sub>–NO interaction under low-temperature conditions. The oxidation process of neat NH<sub>3</sub> and NH<sub>3</sub> doped with NO (450, 800 ppm) was experimentally investigated in a Jet Stirred Flow Reactor at atmospheric pressure for the temperature range 900–1350 K. Results showed NO concentration is entirely controlled by DeNO<sub>x</sub> reactions in the temperature range 1100–1250 K, while NH<sub>3</sub>–NO interaction does not develop through a sensitizing NO effect, for these operating conditions.

A detailed kinetic model was developed by systematically updating rate constants of controlling reactions and declaring new reactions for N<sub>2</sub>H<sub>2</sub> isomers (*cis* and *trans*). The proposed mechanism well captures target species as NO and H<sub>2</sub> profiles. For NH<sub>3</sub>–NO mixtures, NO profiles were properly reproduced through updated DeNO<sub>x</sub> chemistry, while NH<sub>2</sub> recombination reactions were found to be essential for predicting the formation of H<sub>2</sub>. The role of ammonia as a third-body species is implemented in the updated mechanism, with remarkable effects on species predictions. For neat NH<sub>3</sub> mixture, the reaction H+O<sub>2</sub>(+M)=HO<sub>2</sub>(+M) was crucial to predict NO formation *via* the reaction NH<sub>2</sub>+HO<sub>2</sub>=H<sub>2</sub>NO+OH.

© 2022 The Combustion Institute. Published by Elsevier Inc. All rights reserved.

**Keywords:** Ammonia oxidation; NO reduction; Kinetic modeling; Nitrogen chemistry

## 1. Introduction

The compelling requirement to reduce greenhouse gasses emissions has led the scientific com-

munity to explore alternative energy sources, in particular energy vectors with a minor impact on the environment [1,2]. In this context, the processes of thermo-conversion of ammonia as a hydrogen carrier and as a fuel itself are currently research subject matter. While the advantages of using ammonia as a fuel are indisputable in terms of mature production technologies, economical storage and transport infrastructures [3], with respect to hydro-

\* Corresponding author.

E-mail address: [mariavirginia.manna@unina.it](mailto:mariavirginia.manna@unina.it) (M.V. Manna).

gen, its combustion properties, as well as the high potential NO<sub>x</sub> emissions, represent critical drawbacks for conventional combustion processes.

Recent studies [4,5] have demonstrated that MILD combustion [6] processes can allow overcoming these limits, thus simultaneously ensuring stable combustion conditions and low NO<sub>x</sub> emissions. MILD combustion envisages the internal or external recirculation of hot-gasses to increase mixtures heat capacity and control system temperatures, thus pollutants emissions. Under these operative conditions the interaction between fuel and NO has to be carefully addressed, as such species can have a sensitizing effect on fuel oxidation chemistry itself. In addition, MILD combustion working temperatures are compatible with DeNO<sub>x</sub> chemistry [7,8]. Therefore, the interaction between NH<sub>3</sub> and NO becomes a crucial aspect to investigate for both fuel oxidation and NO formation/reduction chemistry.

Dagaut [9] performed experimental and numerical investigation on highly diluted NH<sub>3</sub>–NO mixtures in a Jet Stirred Flow Reactor (JSFR), for several initial concentration of NH<sub>3</sub> and NO, for various equivalent ratios (0.1, 2) at atmospheric pressure in the temperature range 1100–1450 K. The author claimed a mutual sensitization between NH<sub>3</sub> and NO, with a strong interaction on the DeNO<sub>x</sub> chemistry.

Recently, Alzueta et al. [10] have addressed the interaction between NH<sub>3</sub> and NO in a quartz tubular flow reactor at atmospheric pressure and temperatures in the range 700–1500 K, from fuel-lean to -rich conditions. They found that the reduction of NO occurs efficiently at almost any equivalence ratio, with a marginal sensitivity on the NH<sub>3</sub>/NO ratio. The authors identified NH<sub>2</sub>+NO as controlling pathway with a non-significant sensitization effect between these species.

Despite these scientific contributions, the NH<sub>3</sub> oxidation, NO formation/reduction chemistry and the NH<sub>3</sub>–NO interaction are still not properly addressed, especially under low temperatures (< 1400 K). Regarding the NO formation/reduction chemistry, Sabia et al. [11] and Manna et al. [12,13] performed extensive experimental campaigns in a Jet Stirred Flow Reactor (JSFR) for ammonia mixtures in the temperature range 900–1350 K. Results showed NO profiles exhibited a non-monotonic trend as a function of the mixture pre-heating temperature, independently of mixture equivalence ratio. Numerical simulations performed with several mechanisms available in the scientific literature were not able to predict this behavior, due to the high uncertainty in reaction rate constants at low temperatures. In particular, the authors argued that the H<sub>2</sub> concentration profile is also a critical target for modeling ammonia chemistry at low temperatures, as it is a pivotal parameter for tuning the overall system reactivity. In conclusion, the discrepancies between the different kinetic

Table 1  
Experimental operating conditions.

Conditions	Range
Inlet temperature ( $T_{in}$ )	900–1350 K
Equivalence ratio ( $\phi$ )	0.8
Residence time ( $\tau$ )	0.21 s
Pressure ( $P$ )	1.4 atm
Dilution level ( $d$ )	86% in N <sub>2</sub>
NO initial concentration	0, 450, 800 ppm

model predictions are expected as the experimental database for ammonia oxidation is not yet broad enough, particularly at low temperatures. Uncertainties are found in the rate kinetic data. More low-temperature experimental data are needed to allow further improvement of the kinetic models. Several researchers have already put their effort into the development of an NH<sub>3</sub>–NO<sub>x</sub> kinetic model but still, a well-established and reliable model is not available.

The present paper takes up the momentum created by the above-mentioned issues with the aim of providing for:

1. New experimental insights into NH<sub>3</sub>–NO oxidation chemistry in a JSFR;
2. An updated version of the model by Shrestha et al. [14] mechanism able to properly describe NH<sub>3</sub> oxidation and NH<sub>3</sub>–NO interaction chemistry, on the basis of new and experimental literature data.

## 2. Experimental setup

Experimental data were collected using a fused-silica JSFR (volume 113 cm<sup>3</sup>). Its detailed description is reported in the Supplementary Material, Section D. Experiments were performed for NH<sub>3</sub>–NO/O<sub>2</sub> mixtures diluted in N<sub>2</sub> at 86% as a function of the inlet temperature ( $T_{in}$ ) in the range 900–1350 K, under nearly atmospheric pressure (1.4 atm) and a fixed residence time ( $\tau$ ) equal to 0.21 s. The mixture equivalence ratio ( $\phi$ ), defined based on the reaction  $4\text{NH}_3 + 3\text{O}_2 \rightarrow 2\text{N}_2 + 6\text{H}_2\text{O}$ , was 0.8 for all the experimental cases. First, experiments were performed for pure NH<sub>3</sub>, as the reference case, then they were repeated for NH<sub>3</sub>–NO mixtures, with initial contents of NO equal to 450 and 800 ppm. N<sub>2</sub>–NO calibrated gas cylinders were used to feed NO.

The experimental operating conditions are summarized in the Table 1. Each experiment was repeated at least three times under the same operating conditions and verified also in different days.

The reactor temperature was monitored by two thermocouples (N-, R-type) to minimize temperature measurement errors. The maximum error for the temperature measurement is  $\pm 5$  K. The exit gases were analyzed through a gas-chromatograph (Agilent 3000) to detect O<sub>2</sub>, H<sub>2</sub> and N<sub>2</sub>. The maxi-

maximum relative errors for  $O_2$  and  $H_2$  species are below  $\pm 3\%$  (molar fraction). An online analyzer (TESTO 350) was installed to continuously monitor  $NO_x$  concentrations, with a maximum estimated error equal to  $\pm 2$  ppm for NO in the range of 0–100 ppm and  $\pm 5\%$  in the range of 100–500 ppm.

Experimental results were simulated using the PSR code of LOGEresearch [15] and the model provided by Shrestha et al. in [14], derived from a previous version [16]. This mechanism was chosen as the base model since it was validated for several experimental conditions (e.g. laminar flame speed, ignition delay time, speciation).

The reference kinetic scheme was further updated to address the discrepancies with experimental data from the present and previous works by Sabia et al. [11] and Manna et al. [12]. The mechanism was then validated with respect to literature data [9,10,17]. Herein, the Shrestha et al. [14] kinetic mechanism is referred as “Shrestha model”, while the modified version as “updated model”.

For completeness, further kinetic models [18–20] available in the scientific literature were used for comparison (reported as Supplementary Material).

### 3. Kinetic model update

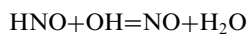
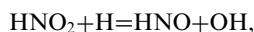
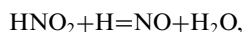
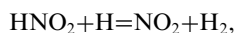
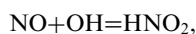
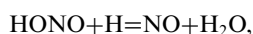
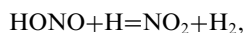
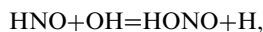
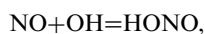
The updated model was systematically built up considering recently updated rate constants and declaring new reactions subsets to reproduce target species profiles, as  $H_2$  and NO, based on new experimental (this work) and scientific literature data [9,10,17], with a peculiar focus on experimental evidences on the  $NH_3$ –NO interaction, congruently with the aim of this work. The updated reactions are briefly discussed in the following.

$NH_2+NO$  is a well-known DeNO<sub>x</sub> reaction with two different pathways: a chain propagating ( $NH_2+NO=NNH+OH$ ) and a chain terminating route ( $NH_2+NO=N_2+H_2O$ ). Their rate constants were updated on the basis of shock tube experiments by Song et al. [21]. They proposed rate constants for temperatures in the range 200–2500 K. Model predictions for  $NH_3$ –NO mixtures significantly improved using these rate constants (see Section 4). These reactions were also crucial to correctly predict pure ammonia oxidation (e.g. laminar flame speed and ignition delay time). Similarly,  $NH_2$  and  $NO_2$  may react forming either  $H_2NO+NO$  or  $N_2O+H_2O$ . Their reaction rates have been adopted from the theoretical work by Glarborg et al. [18].

The reaction  $H_2NO+O_2=HNO+HO_2$  has been recognized as crucial for the low-temperature chemistry of ammonia. In the present study its rate constant is adopted from the recent theoretical work by Cañas et al. [22], with rate constant recommended for temperatures in the range 500–1700 K. The rate constants for some reactions of the HNO sub-mechanism, namely

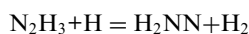
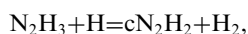
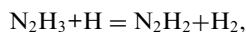
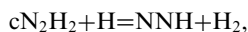
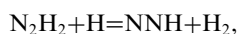
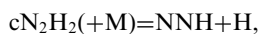
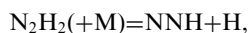
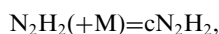
$HNO=H+NO$ ,  $HNO+OH=NO+H_2O$  and  $HNO+NO_2=HNO_2+NO$ , were adopted from a recent work by Stagni et al. [19]. They corrected the reaction rate coefficients of the above-mentioned reactions using experimental and theoretical (*ab initio* method) studies.

Chen et al. [23] performed a detailed investigation of HONO and  $HNO_2$  isomerization and decomposition. State-of-the-art electronic structure theory was used to compute  $HNO_2$  potential energy surface, while temperature and pressure dependent rate coefficients were calculated through micro-canonical rate theory and master equation. The rate constants from [23] for reactions:



were improved in the updated kinetic scheme.

Recently, Marshall et al. [24] investigated the diazene ( $HNNH$ ) oxidation chemistry through the density function theory, including its isomers (*trans*  $N_2H_2$  and *cis*  $cN_2H_2$ ). Both these species were declared in the mechanism, with their relative thermodynamic coefficients, including reactions:



These reactions proved to be very sensitive to the conditions investigated in this work as well as to pure ammonia oxidation, specifically for the prediction of  $H_2$  concentration.

$NH_3+NH_2=N_2H_3+H_2$  (see Section 4) was revealed to be a fundamental reaction to correctly

predict both  $H_2$  and NO profiles, under the conditions considered in this work. Notably, this reaction is not conventionally included in the most recently published ammonia mechanisms. Rate constants for  $NH_3 + NH_2 = N_2H_3 + H_2$  were proposed by Dove and Nip [25] in 1979 on the basis of results from shock-tube ammonia pyrolysis experiments. Since then, to the best of authors' knowledge, only few works have discussed the impact of this reaction in model predictions. Konnov and De Ruyck [26] studied the influence of  $NH_3 + NH_2 = N_2H_3 + H_2$  in modeling the thermal decomposition of ammonia. Abian et al. [27] investigated the impact of the presence of such reaction to predict  $NH_3$  pyrolysis and they demonstrated that, when it is not included in the mechanism, the predicted onset of reactivity occurs at much higher temperatures than observed experimentally.

In this work, the rate constants from [25] were adopted and increased by a factor of 2 to achieve reasonable agreement with experimental results. It is worth mentioning that the prediction of  $H_2$  concentrations is a crucial issue given the recent findings on mutual inhibition of ammonia and hydrogen oxidation chemistry [28].

Furthermore,  $NH_3$  and  $N_2H_x$  third-body collisional efficiencies were also declared for all third-body reactions reported in this study. The role of  $NH_3$  as a “strong” collider in third-body reactions was thoroughly discussed by Sabia et al. [29]. They attribute this behavior to its strong physical/chemical properties (large cross-section, strong polarity and polarizability), likewise  $H_2O$ . They also demonstrated numerically that the reaction  $H + O_2(+M) = HO_2(+M)$  is very sensitive when a suitable third-body collisional efficiency is declared for  $NH_3$ . Congruently,  $NH_3$  third-body efficiencies were declared with a value of 12, on the basis of experimental evidences from the authors' previous study [29].

Herein, it is worth highlighting the plausible role of ammonia as a third-body species is another issue not properly addressed in available kinetic models. Recently, also Glarborg et al. [30] underlined the importance of  $NH_3$  as a third-body species.

The updated mechanism consists of 34 species involved in 284 reversible reactions. The complete list of updated reactions can be found in the Supplementary Material (SM).

## 4. Results and discussion

### 4.1. Experimental and numerical results

Fig. 1 shows the concentration profiles of main species ( $O_2$ , NO,  $H_2$ ) detected for pure  $NH_3$  (black symbols) and  $NH_3$ –NO oxidation (green symbols NO=450 ppm, red symbols NO=800 ppm). Model predictions using the updated mechanism are reported with solid lines, while dashed line report the original Shrestha model. Results are plotted

against the reactor temperature at steady state conditions ( $T$ ).

Fig. 1a shows  $O_2$  profiles for all the considered mixtures. In general,  $O_2$  concentration starts decreasing for  $T=1100$  K and a significant  $O_2$  conversion is observed for  $T>1300$  K. It can be observed that doping the mixture with NO does not alter significantly the system reactivity. It can be noticed that both the Shrestha and the updated model reproduce the experimental trend. However, the former model predicts higher reactivity compared to the latter one for inlet temperature in the range 1200–1280 K. Conversely, the updated model reproduces better experimental data above 1300 K.

The NO trend in Fig. 1b (semilogarithmic scale) for pure  $NH_3$  is peculiarly non-monotonic at low temperatures, in agreement with [11,12]. NO concentrations increase up to 50 ppm at  $T=1150$  K, and then decrease down to a minimum value (30 ppm) for  $T$  around 1250 K.

Afterwards, they increase again with  $T$ . For  $T=1380$  K, NO is about 160 ppm. It can be observed that the updated mechanism satisfactorily predicts the non-monotonic NO experimental trend, in contrast to Shrestha model. Computations using other recently published models [18–20] were also compared against these experimental data (see Fig. S1 in SM). Similarly to the Shrestha model, none of these mechanisms could predict the non-monotonic behavior of NO.

For mixtures doped with NO, the concentration of NO remains equal to the initial value for  $T<1000$  K, while an abrupt NO concentration decrease occurs for  $T$  close to 1100 K, independently of NO initial concentration, suggesting the occurrence of fast  $DeNO_x$  reactions ( $NH_2 + NO = NNH + OH$  and  $NH_2 + NO = N_2 + H_2O$ ). For  $T>1150$  K, regardless of the initial NO concentration in the mixture, NO profiles almost overlap. At higher temperatures,  $DeNO_x$  reactions are less favored, thus NO formation routes overcome, determining a NO concentration increase.

The proposed mechanism reproduces the NO trend very well in the investigated temperature range for both neat  $NH_3$  and NO-doped mixtures. In contrast, Shrestha and other mechanisms (Fig. S1 in SM) fail to predict the NO production and/or reduction.

Hydrogen concentration trends are shown in Fig. 1c. Pure  $NH_3$  and NO-doped mixtures exhibit the same hydrogen trend.  $H_2$  concentrations start increasing for  $T$  around 1000 K and peak at  $T=1150$  K, then they decrease with  $T$ . It can be observed that the Shrestha model predicts a lower hydrogen net production with respect to the experimental data, while the updated model more reasonably captures the conspicuous  $H_2$  formation. For  $T>1300$  K, a very good agreement with experiments can be observed for both the models, suggesting  $NH_3$  low-temperature oxidation chem-

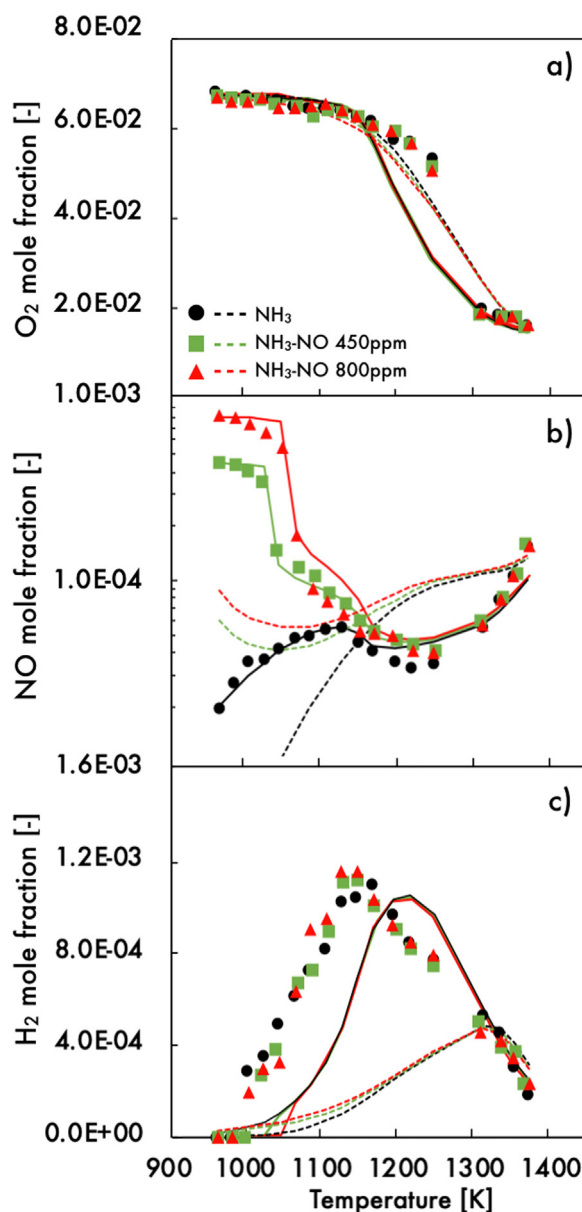


Fig. 1. Experimental (symbols) and model predictions (lines) species profiles for  $\text{NH}_3$  and  $\text{NH}_3\text{-NO}$  mixtures oxidation. Solid lines: updated model, Dashed lines: Shrestha model.

istry is not well described in contrast with the high-temperature one. As matter of facts, the improvement in model prediction of  $\text{H}_2$  trend is mainly due to the update and inclusion of new reactions, particularly involving  $\text{NH}_2$  and  $\text{N}_2\text{H}_x$  species, as discussed in Section 3.

#### 4.2. Kinetic analyses

In order to understand the controlling reactions of  $\text{NH}_3$  oxidation chemistry under the consid-

ered operative conditions, flux diagrams and sensitivity analyses were performed for both the pure ammonia and the NO-doped mixtures (specifically 800 ppm NO), using the updated model.

Fig. 2 shows flux diagrams based on N-atom for three temperatures, namely 1080, 1250 and 1350 K, as representative values for the three different temperature windows with the controlling chemistries, deducible from characteristic non-monotonic species trends ( $\text{NO}$ ,  $\text{H}_2$ ). Line thickness is proportional to the reaction rate (shown in round



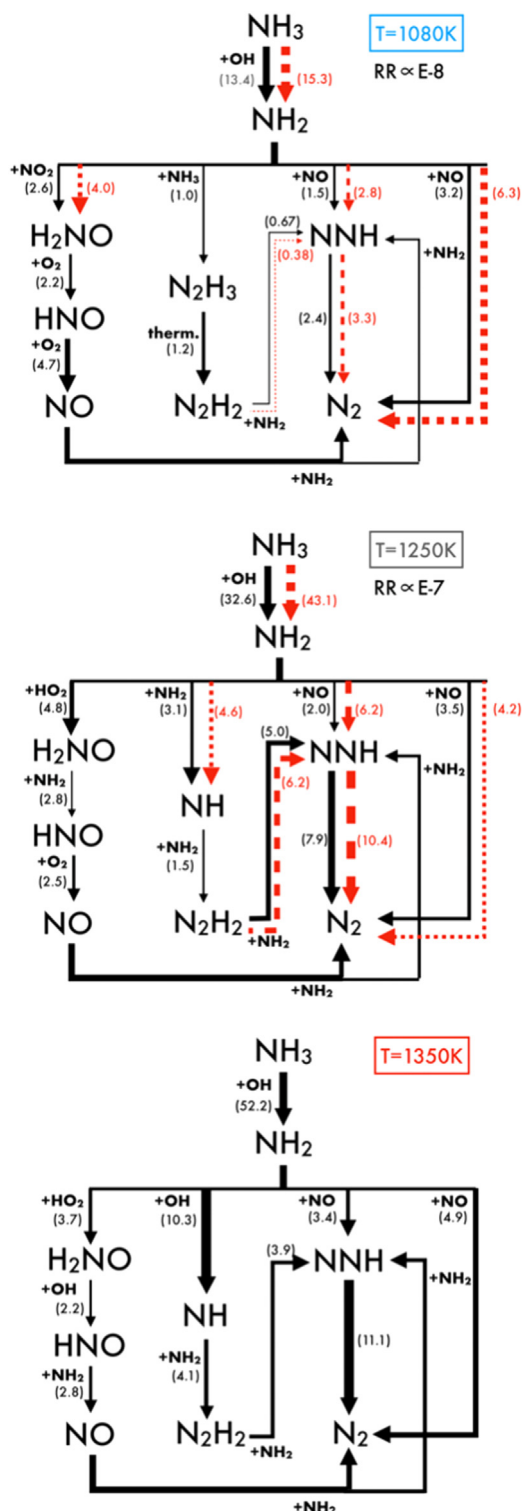


Fig. 2. Flux diagrams analyses for  $\text{NH}_3$  and  $\text{NH}_3\text{-NO}$  oxidation. Solid lines: main pathways for pure  $\text{NH}_3$ . Dashed lines: effect of 800 ppm NO addition on the main pathways.

brackets). Dashed arrows are relative to reactions more markedly affected by NO as an inlet species. Congruently, they are not shown when negligible.

NH<sub>3</sub> exclusively yields NH<sub>2</sub> by reacting with OH radicals. The formed NH<sub>2</sub> reacts with HO<sub>2</sub>, OH and NO to yield H<sub>2</sub>NO, NH, NNH and N<sub>2</sub>, depending on the temperature. At 1080 K, H<sub>2</sub>NO is formed *via* reactions NH<sub>2</sub>+NO<sub>2</sub>=H<sub>2</sub>NO+NO and NH<sub>2</sub>+HO<sub>2</sub>=H<sub>2</sub>NO+OH (the latter not reported in the diagram for clearness). Secondly, NH<sub>2</sub> is involved in DeNO<sub>x</sub> reactions (NH<sub>2</sub>+NO=N<sub>2</sub>+H<sub>2</sub>O, NH<sub>2</sub>+NO=NNH+OH). Specifically, at low temperatures, the terminating reaction NH<sub>2</sub>+NO=N<sub>2</sub>+H<sub>2</sub>O is faster than the propagating one, NH<sub>2</sub>+NO=NNH+OH. The H<sub>2</sub>NO is involved in NO formation according to the pathway H<sub>2</sub>NO→HNO→NO, then NO is partially reduced to N<sub>2</sub>. NH<sub>2</sub> recombination pathway to N<sub>2</sub>H<sub>3</sub> accounts only for 5% of NH<sub>2</sub> net reactions.

Nonetheless  $\text{H}_2$  formation is very sensitive to the  $\text{N}_2\text{H}_x$  pathway. In particular, the reaction  $\text{NH}_3 + \text{NH}_2 = \text{N}_2\text{H}_3 + \text{H}_2$  is responsible for the  $\text{H}_2$  production at low-intermediate temperatures.  $\text{H}_2$  consumption through the typical  $\text{H}_2/\text{O}_2$  oxidation chemistry is partially inhibited by  $\text{NH}_3$  itself, since its third-body efficiency enhances the role of the chain terminating reaction  $\text{H} + \text{O}_2 (+\text{M}) = \text{HO}_2 (+\text{M})$ , thus delaying the high-temperature branching mechanism ( $\text{H} + \text{O}_2 = \text{OH} + \text{O}$ ) [29]. In addition, due to the importance of such reaction, the  $\text{HO}_2$  formation is promoted for low-intermediate temperatures, thus simultaneously boosting NO production.

As the temperature increases ( $T=1250$  K), the relative balance of oxidative, recombination and  $\text{DeNO}_x$  pathways changes. Indeed,  $\text{NH}_2$  is mainly involved in NH formation, that subsequently recombines with  $\text{NH}_2$  to  $\text{N}_2\text{H}_2$ . The pathway  $\text{NH} \rightarrow \text{N}_2\text{H}_2 \rightarrow \text{NNH} \rightarrow \text{N}_2$  promotes the formation of  $\text{H}_2$  and H radicals, thus enhances the system reactivity. Moreover, the reactions  $\text{NH}_2 + \text{NO}$  become predominant compared to  $\text{H}_2\text{NO}$  formation *via*  $\text{NH}_2 + \text{HO}_2 = \text{H}_2\text{NO} + \text{OH}$ . As a consequence, NO formation is slowed down in favor of its consumption, resulting in a net NO decrease with temperature from  $T=1150$  K up to 1250 K, as shown in Fig. 1.

For higher temperatures ( $T = 1350$  K), the  $\text{H}_2/\text{O}_2$  branching mechanism boosts OH formation, thus the high temperature reactivity is dominated by the conversion of  $\text{NH}_2$  to  $\text{NH}$ , according to the reaction  $\text{NH}_2 + \text{OH} = \text{NH} + \text{H}_2\text{O}$ , while the  $\text{H}_2\text{NO}$  formation and the  $\text{DeNO}_x$  reactions play a secondary role. Therefore,  $\text{NH}$  is mainly consumed through the recombination pathway to  $\text{N}_2\text{H}_2$ . In addition, the  $\text{NH}$  paths also contribute to  $\text{NO}$  formation, along with the  $\text{H}_2\text{NO}/\text{HNO}$  reactions, since  $\text{NH}$  reacts with  $\text{O}_2$  and the  $\text{OH}$  radicals to directly produce  $\text{NO}$ . Overall, albeit the increased reaction rate of the  $\text{NO}$  consumption, such

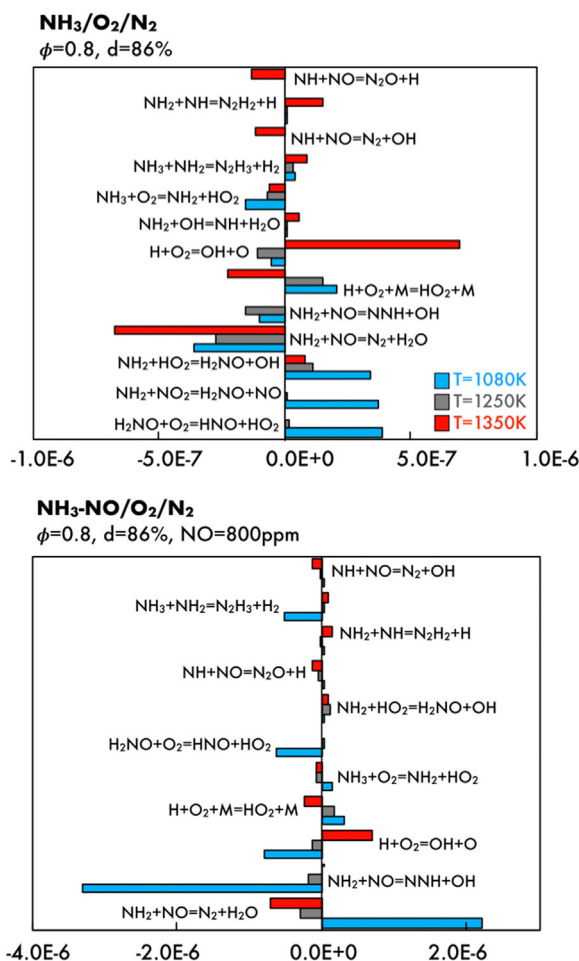


Fig. 3. NO sensitivity analyses for NH<sub>3</sub> and NH<sub>3</sub>-NO oxidation at three different temperatures.

new pathways to NO formation lead to an increase of NO concentration with temperature.

The major impact of NO addition to NH<sub>3</sub> oxidation pathways is observed for low and intermediate temperatures. At  $T=1080$  K, the reaction  $\text{NH}_2+\text{NO}=\text{N}_2+\text{H}_2\text{O}$  prevails over both the chain propagating one ( $\text{NH}_2+\text{NO}=\text{NNH}+\text{OH}$ ) and the  $\text{H}_2\text{NO}$  formation, resulting in a slight decrease of NO concentration, without significant effect on the overall system reactivity, congruently with experimental results. As the temperature increases ( $T=1250$  K), the reaction  $\text{NH}_2+\text{NO}=\text{NNH}+\text{OH}$  becomes faster than the terminating one, enhancing the formation of both OH and H radicals, the latter mainly formed *via* NNH unimolecular dissociation route ( $\text{NNH}=\text{N}_2+\text{H}$ ).

The NO formation and consumption were also investigated by sensitivity analyses, performed for the pure ammonia and NO doped cases, at 1080, 1250 and 1350 K.

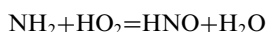
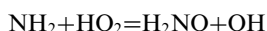
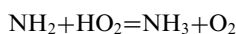
The analyses are reported in Fig. 3. Positive sensitivity means that the reaction promotes the NO formation and vice versa for negative sensitivity. In line with the flux diagrams (Fig. 2), at low and intermediate temperatures, the most sensitive reactions for NO production are the reactions involving  $\text{H}_2\text{NO}$  ( $\text{NH}_2+\text{NO}_2=\text{H}_2\text{NO}+\text{NO}$ ,  $\text{NH}_2+\text{HO}_2=\text{H}_2\text{NO}+\text{NO}$ ) and its conversion to HNO ( $\text{H}_2\text{NO}+\text{O}_2=\text{HNO}+\text{HO}_2$ ). The reaction  $\text{NH}_3+\text{O}_2=\text{NH}_2+\text{HO}_2$  inhibits the NO formation at low temperature, as suggested by its negative sensitivity coefficient.

Due to its relevance to the NO formation path, the production of  $\text{HO}_2$  via  $\text{H}+\text{O}_2(+\text{M})=\text{HO}_2(+\text{M})$  has a positive sensitivity coefficient. Its role in NH<sub>3</sub> oxidation and speciation is even emphasized by the declaration of a high third-body collisional efficiency for NH<sub>3</sub> and other nitrogen species (e.g.,  $\text{N}_2\text{H}_2$ ,  $\text{N}_2\text{H}_4$ ), as further demonstrated in the Supplementary Material,

Section C. The same reactions exhibit lower sensitivity coefficients for  $\text{NH}_3$ –NO oxidation. In this case,  $\text{DeNO}_x$  reactions are predominant. Indeed, they show high negative sensitivity coefficients for low-intermediate temperatures.

At higher temperature conditions for the investigated mixtures, the reaction  $\text{NH}_2 + \text{NO} = \text{N}_2 + \text{H}_2\text{O}$  shows the highest negative sensitivity as it consumes NO. Furthermore, the NO formation is very sensitive to chain branching reaction  $\text{H} + \text{O}_2 = \text{OH} + \text{O}$ .

In general, for low-intermediate temperatures, the prediction of the peculiar non-monotonic trend of NO depends on the balance between the  $\text{DeNO}_x$  pathway and the different product channels of the reaction  $\text{NH}_2 + \text{HO}_2$ . Literature studies suggest that the following reactions:



are the main product channels of  $\text{NH}_2 + \text{HO}_2$ . Nonetheless, the theoretical study of Xiang et al. [31] demonstrated that  $\text{NH}_2 + \text{HO}_2 = \text{HNO} + \text{H}_2\text{O}$  is a minor pathway. Theoretical calculations by Stagni et al. [19] indicated that the reverse reaction of  $\text{NH}_2 + \text{HO}_2 = \text{NH}_3 + \text{O}_2$  is faster than previous calculations. The room temperature value of  $\text{NH}_3 + \text{O}_2 = \text{NH}_2 + \text{HO}_2$  recently calculated by Glarborg et al. [30] is in good agreement with the work of Stagni et al.

Nevertheless, despite the evidence *via* theoretical calculations suggests  $\text{NH}_3 + \text{O}_2$  is the main product channel of  $\text{NH}_2 + \text{HO}_2$ , it is worth underlining that the experimental evaluation of the kinetic constants of such reaction is problematic due to simultaneous occurrence of side reactions involving  $\text{NH}_2$  radical as indicated by the flash photolysis experiments of  $\text{NH}_3/\text{O}_2$  mixtures [32]. Moreover, for the reverse reaction of  $\text{NH}_2 + \text{HO}_2 = \text{NH}_3 + \text{O}_2$  Stagni et al. [19] found a strong temperature-dependence, decreasing more than a factor of five as the temperature increases up to 2000 K. Therefore, a significant uncertainty margin has to be considered for of  $\text{NH}_2 + \text{HO}_2$ , especially concerning the temperature dependence of the overall reaction and the branching fraction of the different product channels [30]. Considering such uncertainty, therefore in the present study the rate constant of  $\text{NH}_2 + \text{HO}_2$  product channel has been modified to have a better agreement with the present measurements.

Another critical aspect that is worth stressing is the prediction of  $\text{H}_2$  trend at low-intermediate temperatures. As argued in previous works [11,12] and confirmed by the kinetic analyses on the basis of the present model,  $\text{H}_2$  is formed mainly from  $\text{NH}_3$  pyrolytic pathways, that include both recombination and decomposition reactions. Therefore, the effect of reactions involving  $\text{NH}_2$  and

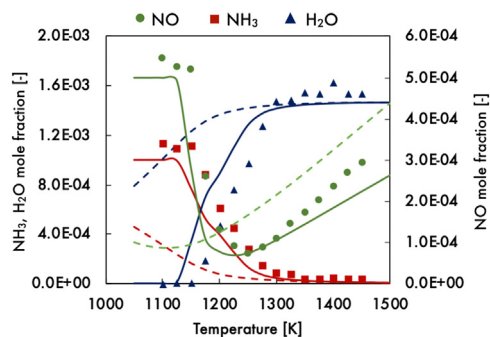


Fig. 4. Experimental data from Dagaut [9] and numerical species profiles with the proposed mechanism (solid lines) and Shrestha 2021 mechanism (dashed lines).

$\text{N}_2\text{H}_x$  radicals on  $\text{H}_2$  formation was extensively studied. In particular, including reactions involving *cis*- $\text{N}_2\text{H}_2$  and *trans*- $\text{N}_2\text{H}_2$  species together with the reaction  $\text{NH}_3 + \text{NH}_2 = \text{N}_2\text{H}_3 + \text{H}_2$  considerably improved the model predictions for  $\text{H}_2$ . Indeed, based on the updated mechanism, kinetic analyses showed that at 1080 K,  $\text{H}_2$  is mainly formed *via*  $\text{NH}_3 + \text{NH}_2 = \text{N}_2\text{H}_3 + \text{H}_2$ , while its role becomes marginal as the temperature increases ( $T > 1250$  K).

The reaction  $\text{NH}_3 + \text{NH}_2 = \text{N}_2\text{H}_3 + \text{H}_2$  has been largely ignored and thus not included in most of recent detailed kinetic models for  $\text{NH}_3$  oxidation. Only few works discuss the impact of this reaction in model predictions. Nonetheless, due to the proven sensitivity of this reaction, further experimental and theoretical studies are warranted.

#### 4.3. Model validation against literature data

The performance of the proposed mechanism has been further evaluated against different literature data for  $\text{NH}_3$ –NO interaction (JSFR and tubular flow reactor) and  $\text{NH}_3$  oxidation (laminar flame speed and ignition delay time).

Fig. 4 illustrates the comparison between model predictions against the experimental data by Dagaut [9]. The author [9] investigated  $\text{NH}_3$ –NO oxidation in a JSFR for different equivalence ratios (0.1, 2) and various initial concentration of  $\text{NH}_3$  and NO (500 and 1000 ppm), under atmospheric pressure. For brevity, only the case at  $\phi = 0.1$  and NO initial concentration equal to 500 ppm is shown. The comparison for the other conditions is reported in the Supplementary Material, Section B.  $\text{NH}_3$  and  $\text{H}_2\text{O}$  concentrations refer to the primary axis, while NO concentration is plotted on the secondary axis.

Both the numerical results obtained with the updated and Shrestha models are reported. It can be observed that the prediction of the proposed model was considerably improved compared to Shrestha model. Indeed, it reproduces all the species trends



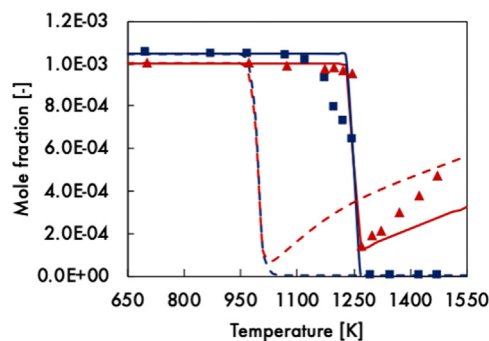


Fig. 5. Experimental data from Alzueta et al. [8] and numerical species profiles with the current mechanism (solid lines) and Shrestha mechanism (dashed lines).

well, within the experimental uncertainty in the whole temperature range.

In particular, for such operative conditions the mechanism predictions are very sensitive to the DeNO<sub>x</sub> reactions. Therefore, the better agreement between data and simulations can be ascribed to the implementation of updated kinetic parameters for the reactions NH<sub>2</sub>+NO.

Similar improvements were achieved for the prediction of the experimental data from Alzueta et al. [10] (Fig. 5). They investigated NH<sub>3</sub>–NO oxidation in a flow reactor, at atmospheric pressure, in the temperature range 700–1500 K, for various air excess ratio ( $\lambda=1.65, 1.01, 0.5$ ) and NH<sub>3</sub>/NO ratio in the range 0.7–3.5. The results herein reported refer to  $\lambda=1.65$  ( $\phi=0.6$ ), while the species profiles for other air excess ratios are presented in the SM.

The proposed mechanism well captures NH<sub>3</sub> and NO profiles in the investigated temperature range, whereas Shrestha mechanism predicts an overall increased reactivity compared to the experimental data. The updated model in this work is also tested against other experimental data i.e. laminar flame speed and ignition delay times for pure ammonia mixtures. The model shows a good agreement with these experimental data as well. The complete comparison for such operative conditions is reported in the SM.

## 5. Conclusions

The present paper deals with an experimental and modeling study on the oxidation of NH<sub>3</sub> and NH<sub>3</sub>–NO mixtures. Experiments were performed in a Jet Stirred Flow Reactor, for mixtures diluted in N<sub>2</sub> at 86%, doped with 450 and 800 ppm of NO, in the temperature range 900–1350 K. Under these operative conditions, NH<sub>3</sub>–NO interaction does not develop through a sensitizing effect, as O<sub>2</sub> and H<sub>2</sub> profiles are not influenced by NO as an inlet species. The NO profile for pure ammonia exhibits a peculiar non-monotonic trend, in agreement with previous results. For NH<sub>3</sub> and

NH<sub>3</sub>–NO mixtures, NO concentrations are controlled by DeNO<sub>x</sub> reactions in the temperature range 1100–1250 K. Based on these measurements, a detailed kinetic mechanism was developed updating the Shrestha et al. [14] model, systematically considering recently updated rate constants and declaring new reactions subsets, relevant for ammonia low-temperature oxidation chemistry, to properly reproduce target species profiles (H<sub>2</sub> and NO). The updated mechanism was validated against the literature experimental data for NH<sub>3</sub>–NO oxidation in flow reactors, laminar flames and ammonia ignition delay times.

Numerical analyses show the low-temperature chemistry of ammonia is predominantly controlled by the H<sub>2</sub>NO formation and consumption pathways. However, at high temperature, the decomposition route of NH<sub>2</sub> (NH<sub>2</sub>→NH→N<sub>2</sub>H<sub>2</sub>→NNH→N<sub>2</sub>) controls the oxidation process, leading to the formation of H<sub>2</sub> and H radicals, enhancing the system reactivity. Moreover, the role of the NH<sub>2</sub>+NO reactions becomes marginal at high temperature, and therefore the oxidation process is not affected by the NO addition. In particular, model advancements are ascribable to updated rate constants of DeNO<sub>x</sub> reactions. The proper description of H<sub>2</sub> concentration relies on the declaration of new reactions relative to NH<sub>2</sub> recombination to N<sub>2</sub>H<sub>x</sub> species and their relative decomposition. Significantly, the role of ammonia as a strong collider has been included, declaring a high collisional efficiency in third-body reactions.

## Declaration of Competing Interest

-All authors have seen and approved the final version of the manuscript being submitted.

-The authors declare there is not any Conflict of Interest.

-The authors declare that they have no known competing financial interests or personal relationships that could have appeared to influence the work reported in this paper.

-The authors declare that they have not received any funding or research grants (and their source) received in the course of study, research or assembly of the manuscript

-The authors declare that all figures and materials used in the manuscript have been produced by themselves thus no permissions are required.

## Supplementary materials

Supplementary material associated with this article can be found, in the online version, at doi:[10.1016/j.proci.2022.09.027](https://doi.org/10.1016/j.proci.2022.09.027).

## References

- [1] P. Sabia, G. Sorrentino, G.B. Ariemma, M.V. Manna, R. Ragucci, M. de Joannon, MILD combustion

- and biofuels : a minireview, *Energy Fuels* 35 (2021) 19901–19919.
- [2] A. Dreizler, H. Pitsch, V. Scherer, C. Schulz, J. Janicka, The role of combustion science and technology in low and zero impact energy transformation processes, *Appl. Energy Combust. Sci.* 7 (2021) 100040.
  - [3] A. Valera-Medina, F. Amer-Hatem, A.K. Azad, I.C. Dedoussi, M. de Joannon, R.X. Fernandes, P. Glarborg, H. Hashemi, X. He, S. Mashruk, J. McGowan, C. Mounaïm-Rousselle, A. Ortiz-Prado, A. Ortiz-Valera, I. Rossetti, B. Shu, M. Yehia, H. Xiao, M. Costa, Review on ammonia as a potential fuel: from synthesis to economics, *Energy Fuels* 35 (2021) 6964–7029.
  - [4] G.B. Ariemma, P. Sabia, G. Sorrentino, P. Bozza, M. De Joannon, R. Ragucci, Influence of water addition on MILD ammonia combustion performances and emissions, *Proc. Combust. Inst.* 38 (2021) 5147–5154.
  - [5] G. Sorrentino, P. Sabia, P. Bozza, R. Ragucci, M. de Joannon, Low-NO<sub>x</sub> conversion of pure ammonia in a cyclonic burner under locally diluted and preheated conditions, *Appl. Energy* 254 (2019) 1–7.
  - [6] A. Cavaliere, M. de Joannon, Mild Combustion, *Prog. Energy Combust. Sci.* 30 (2004) 329–366.
  - [7] U. Asghar, S. Rafiq, A. Anwar, T. Iqbal, A. Ahmed, F. Jamil, M.S. Khurram, M.M. Akbar, A. Farooq, N.S. Shah, Y.K. Park, Review on the progress in emission control technologies for the abatement of CO<sub>2</sub>, SO<sub>x</sub> and NO<sub>x</sub> from fuel combustion, *J. Environ. Chem. Eng.* 9 (2021) 106064.
  - [8] R.K. Lyon, J.E. Hardy, Discovery and development of the thermal DeNO<sub>x</sub> process, *Ind. Eng. Chem. Fundam.* 25 (1986) 19–24.
  - [9] P. Dagaut, On the oxidation of ammonia and mutual sensitization of the oxidation of NO and ammonia: experimental and kinetic modeling, *Combust. Sci. Technol.* 194 (2022) 117–129.
  - [10] M.U. Alzueta, L. Ara, V.D. Mercader, M. Delogu, R. Bilbao, Interaction of NH<sub>3</sub> and NO under combustion conditions. Experimental flow reactor study and kinetic modeling simulation, *Combust. Flame* (2021) 111691.
  - [11] P. Sabia, M.V. Manna, A. Cavaliere, R. Ragucci, M. de Joannon, Ammonia oxidation features in a Jet Stirred Flow Reactor. The role of NH<sub>2</sub> chemistry, *Fuel* 276 (2020) 118054.
  - [12] M.V. Manna, P. Sabia, R. Ragucci, M. de Joannon, Oxidation and pyrolysis of ammonia mixtures in model reactors, *Fuel* 264 (2020) 116768.
  - [13] M.V. Manna, P. Sabia, R. Ragucci, M. de Joannon, Ammonia oxidation regimes and transitional behaviors in a Jet Stirred Flow Reactor, *Combust. Flame* 228 (2021) 388–400.
  - [14] K.P. Shrestha, C. Lhuillier, A.A. Barbosa, P. Brequigny, F. Contino, C. Mounaïm-Rousselle, L. Seidel, F. Mauss, An experimental and modeling study of ammonia with enriched oxygen content and ammonia/hydrogen laminar flame speed at elevated pressure and temperature, *Proc. Combust. Inst.* 38 (2021) 2163–2174.
  - [15] LOGEresearch: combustion and chemical kinetics simulation software, (2021).
  - [16] K.P. Shrestha, L. Seidel, T. Zeuch, F. Mauss, Detailed kinetic mechanism for the oxidation of ammonia including the formation and reduction of nitrogen oxides, *Energy Fuels* 32 (2018) 10202–10217.
  - [17] Y. Song, H. Hashemi, J.M. Christensen, C. Zou, P. Marshall, P. Glarborg, Ammonia oxidation at high pressure and intermediate temperatures, *Fuel* 181 (2016) 358–365.
  - [18] P. Glarborg, J.A. Miller, B. Ruscic, S.J. Klippenstein, Modeling nitrogen chemistry in combustion, *Prog. Energy Combust. Sci.* 67 (2018) 31–68.
  - [19] A. Stagni, C. Cavallotti, S. Arunthanayothin, Y. Song, O. Herbinet, F. Battin-Leclerc, T. Faravelli, An experimental, theoretical and kinetic-modeling study of the gas-phase oxidation of ammonia, *React. Chem. Eng.* 5 (2020) 696–711.
  - [20] X. Zhang, S.P. Moosakutty, R.P. Rajan, M. Younes, S.M. Sarathy, Combustion chemistry of ammonia/hydrogen mixtures: jet-stirred reactor measurements and comprehensive kinetic modeling, *Combust. Flame* 234 (2021) 111653.
  - [21] S. Song, R.K. Hanson, C.T. Bowman, D.M. Golden, J.E. Chavarrio Cañas, M. Monge-Palacios, X. Zhang, S.M. Sarathy, K.P. Shrestha, C. Lhuillier, A.A. Barbosa, P. Brequigny, F. Contino, C. Mounaïm-Rousselle, L. Seidel, T. Zeuch, F. Mauss, Shock tube determination of the overall rate of NH<sub>2</sub>+NO→ products at high temperatures, *Proc. Combust. Inst.* 32 (2022) 2163–2174.
  - [22] J.E. Chavarrio Cañas, M. Monge-Palacios, X. Zhang, S.M. Sarathy, Probing the gas-phase oxidation of ammonia: addressing uncertainties with theoretical calculations, *Combust. Flame* (2021) 111708.
  - [23] X. Chen, M.E. Fuller, C. Franklin Goldsmith, Decomposition kinetics for HONO and HNO<sub>2</sub>, *React. Chem. Eng.* 4 (2019) 323–333.
  - [24] P. Marshall, G. Rawling, P. Glarborg, New reactions of diazene and related species for modelling combustion of amine fuels, *Mol. Phys.* 119 (2021) 17–18.
  - [25] J.E. Dove, W.S. Nip, A shock-tube study of ammonia pyrolysis, *Can. J. Chem.* 57 (1979) 689–701.
  - [26] A.A. Konnov, J. De Ruyck, Kinetic modeling of the thermal decomposition of ammonia, *Combust. Sci. Technol.* 152 (2000) 23–37.
  - [27] M. Abián, M. Benés, A. de Goñi, B. Muñoz, M.U. Alzueta, Study of the oxidation of ammonia in a flow reactor. Experiments and kinetic modeling simulation, *Fuel* 300 (2021).
  - [28] P. Sabia, M. de Joannon, On H<sub>2</sub>–O<sub>2</sub> oxidation in several bath gases, *Int. J. Hydrogen Energy* 45 (2020) 8151–8167.
  - [29] P. Sabia, M.V. Manna, R. Ragucci, M. de Joannon, Mutual inhibition effect of hydrogen and ammonia in oxidation processes and the role of ammonia as “strong” collider in third-molecular reactions, *Int. J. Hydrogen Energy* 45 (2020) 32113–32127.
  - [30] P. Glarborg, H. Hashemi, S. Cheskis, A.W. Jasper, On the rate constant for NH<sub>2</sub>+HO<sub>2</sub> and third-body collision efficiencies for NH<sub>2</sub>+H(+M) and NH<sub>2</sub>+NH<sub>2</sub>(+M), *J. Phys. Chem. A* 125 (2021) 1505–1516.
  - [31] T. Xiang, H. Si, P. Han, Y. Ruan, Theoretical study on the mechanism of the HO<sub>2</sub> plus NH<sub>2</sub> reaction, *Comput. Theor. Chem.* 985 (2012) 67–71.
  - [32] S.G. Cheskis, O.M. Sarkisov, Flash photolysis of ammonia in the presence of oxygen, *Chem. Phys. Lett.* 62 (1979) 72–76.